Volcanic eruptions

Rüdiger Gens

Advantages of InSAR for monitoring natural hazards

Volcanic eruptions

- SAR interferometry provides continuous information covering area of interest
  - choice of studying various deformation models
  - enough information to allow model inversion to verify model results
- cost effective compared to alternative point measurements (GPS, leveling etc.)

InSAR and volcanoes: What can be measured?

Volcanic eruptions

- spatial mapping of line-of-sight displacements over periods from weeks to years
  - finite strain release during an eruption at an otherwise unmonitored volcano
  - inter-eruption strain over several years in the calderas of shield volcanoes
  - surface-strain events above magmatic systems in continental crust with no immediate volcanological context
  - strains interpretable as being due to gravitational spreading forces at the base of a volcano

Constraints of DInSAR for volcano monitoring

- radar system
  - data swath width and spatial resolution
  - wavelength
    - C-band able to detect ~1 cm deformaton, though at times subject to additional scattering
    - L-band less susceptible to vegetation scattering
  - orbit repeat interval
    - repeat-pass cycle (ERS – 35 days, RADARSAT – 24 days) not necessarily sufficient for certain strain rates
  - baselines
    - practical quality threshold for DInSAR baselines: few hundred meters or less

Stevens, N.F. and Wadge, G., 2004. Towards operational repeat-pass SAR interferometry at active volcanoes. *Natural Hazards*, **33**(1): 47-76.

Constraints of DInSAR for volcano monitoring

Volcanic eruptions

- radar system
  - pointing
    - zero Doppler steering preferable acquisition mode (not available for RADARSAT) - less suitable image pairs otherwise
    - loss of gyros on ERS-2 similar impact
  - line of sight
    - DInSAR only measures component of motion along the line of sight
    - imagery from ascending and descending orbits reduce uncertainty of three-dimensional motion
  - data storage and reception
    - volcano location might require on-board recording (RADARSAT) or data relay satellites (ENVISAT) for acquisition

Stevens, N.F. and Wadge, G., 2004. Towards operational repeat-pass SAR interferometry at active volcanoes. *Natural Hazards*, **33**(1): 47-76.

Constraints of DInSAR for volcano monitoring

- surface
  - stability of the surface
    - position and orientation of sub-pixel scatterers (local metric scale topography, rock facets, plants)
    - moisture in the rock or soil (dielectric constant)
    - erosion and volcanic deposits
  - emplacement of volcanic products (lava, ash, debris flows)
    - causes decorrelation of signal

Volcanic eruptions

Stevens, N.F. and Wadge, G., 2004. Towards operational repeat-pass SAR interferometry at active volcanoes. *Natural Hazards*, **33**(1): 47-76.

Constraints of DInSAR for volcano monitoring

Volcanic eruptions

- interpretational constraints
  - simplistic deformation field representation as point source in an elastic half-space (Mogi model) might need further confirmation
    - evidence the signal does not contain atmospheric effects
    - geodetic measurements that validate the single line-of-sight observation representing three-dimensional motion (e.g. GPS)
    - location of the source (e.g., seismic, petrologic) or timing of the motion
    - hydrological/geochemical/gas data on the contemporary behaviour of the hydrothermal system

Stevens, N.F. and Wadge, G., 2004. Towards operational repeat-pass SAR interferometry at active volcanoes. *Natural Hazards*, **33**(1): 47-76.

Constraints of DInSAR for volcano monitoring

- volcano type
  - basaltic shield volcanoes suitable
    - highly active, shallow crustal reservoirs that give a large amplitude ground deformation signal
  - andesitic stratovolcanoes not suitable
    - long repose periods

Stevens, N.F. and Wadge, G., 2004. Towards operational repeat-pass SAR interferometry at active volcanoes. *Natural Hazards*, **33**(1): 47-76.

Example: Ecuador
Seasonal effects on coherence

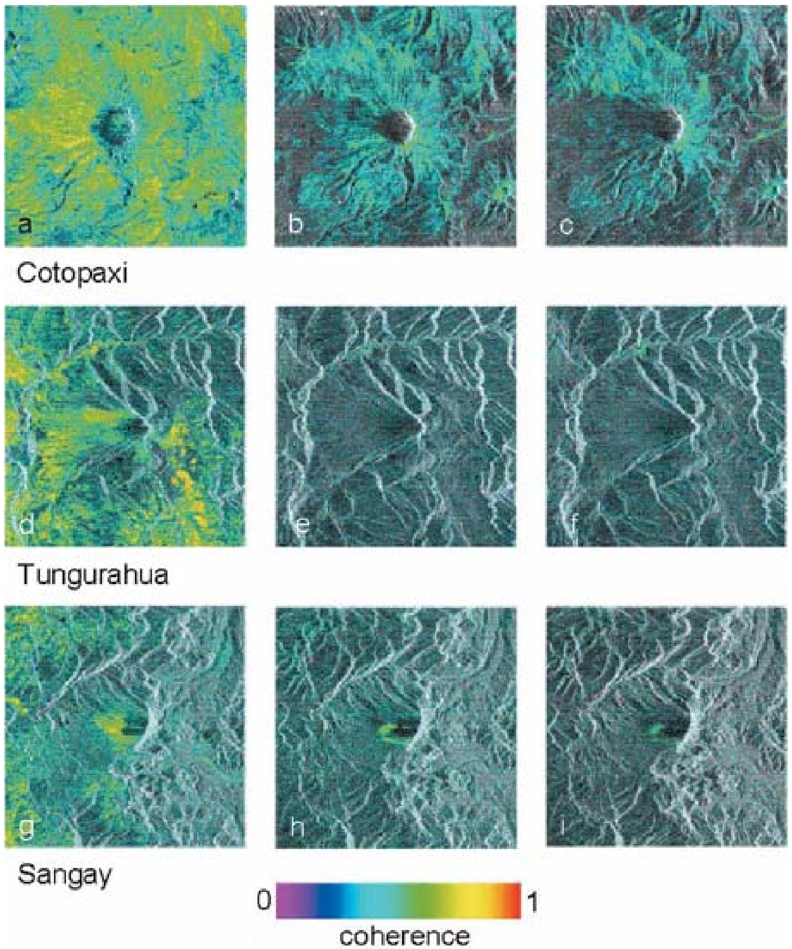

- a, d, g: summer tandem pairs
- b, e, h: summer-fall inter-seasonal (8 months)
- c, f, i: summer inter-annual

- Cotopaxi in arid area
- Tunguraha and Sangay vegetated

Volcanic eruptions

Stevens, N.F. and Wadge, G., 2004. Towards operational repeat-pass SAR interferometry at active volcanoes. *Natural Hazards*, **33**(1): 47-76.

Example: Sierra Negra, Galapagos Different deformation models

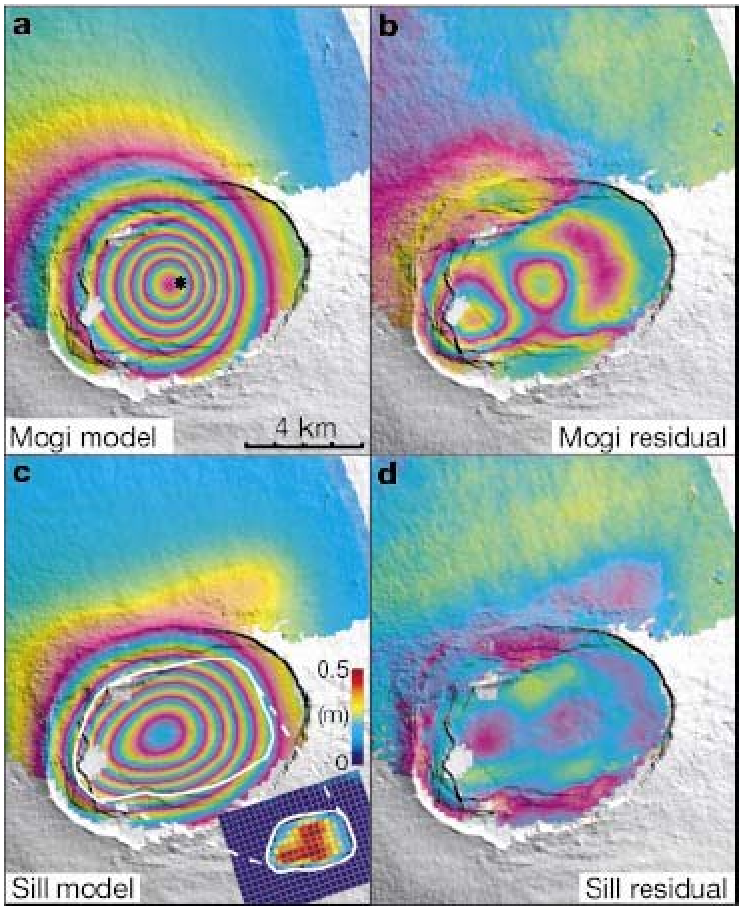

- a, b:
  best-fit Mogi model shows large residuals
- c, d:
  horizontal sill at 1.9 km depth with variable openings of up to 0.5 m

Amelung, F., Jonsson, S., Zebker, H. and Segall, P., 2000. Widespread uplift and 'trapdoor' faulting on Galapagos volcanoes observed with radar interferometry. *Nature*, **407**(6807): 993-996.

Example: Sierra Negra, Galapagos Monitoring processes over time

Volcanic eruptions

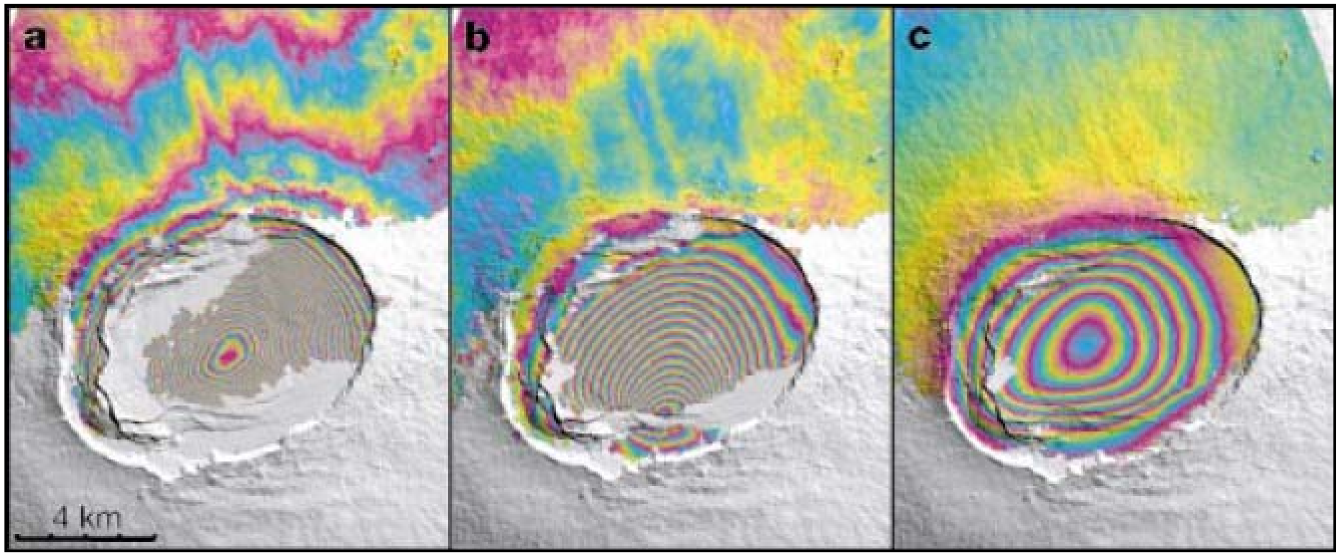

color cycle represents 5 cm line-of-sight displacement

- a: 1992-97 (5.3 years) – uplift
- b: 1997-98 (1.1 years) – suggested trapdoor faulting
- c: 1998-99 (0.5 years) – uplift

Amelung, F., Jonsson, S., Zebker, H. and Segall, P., 2000. Widespread uplift and 'trapdoor' faulting on Galapagos volcanoes observed with radar interferometry. *Nature*, **407**(6807): 993-996.

Example: Mt Etna eruption (1991-93) Combination of data sources

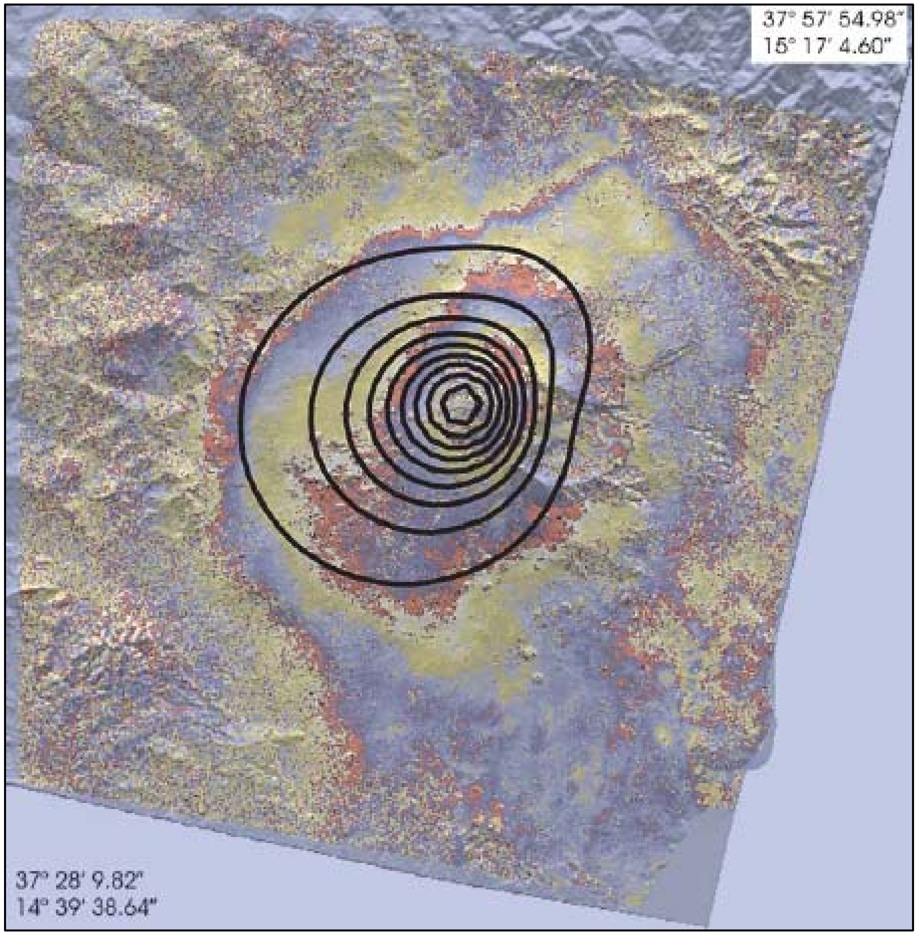

- isolines: deformation pattern from geodetic measurements – first half of eruption
- interferogram: deformation in the line-of-sight (28 mm per fringe) – second half of eruption suggesting a deeper source

Bonaccorso, A., Sansosti, E. and Berardino, P., 2004. Comparison of integrated geodetic data models and satellite radar interferograms to infer magma storage during the 1991-1993 Mt. Etna eruption. *Pure And Applied Geophysics*, **161**(7): 1345-1357

Example: Okmok Alaska Lava thickness estimation

Volcanic eruptions

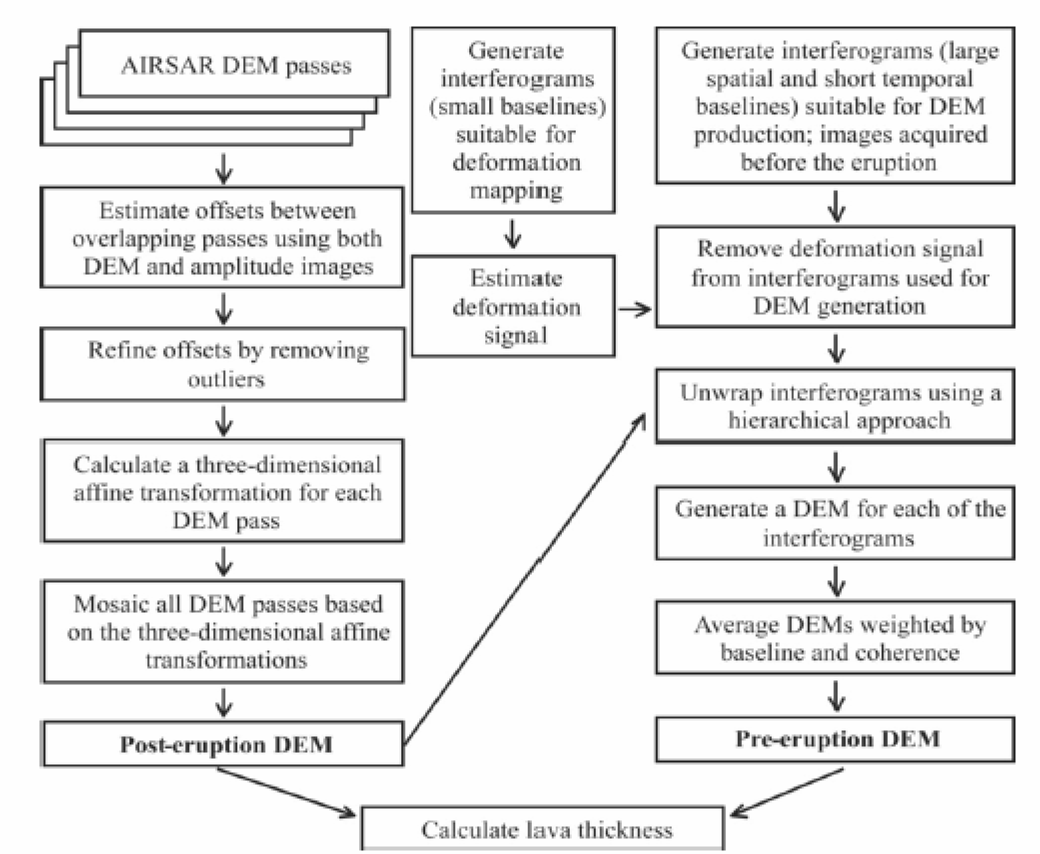

Lu, Z., Fielding, E., Patrick, M.R. and Trautwein, C.M., 2003. Estimating lava volume by precision combination of multiple baseline spaceborne and airborne interferometric synthetic aperture radar: The 1997 eruption of Okmok Volcano, Alaska. *Ieee Transactions On Geoscience And Remote Sensing*, **41**(6): 1428-1436

Example: Okmok Alaska
Lava thickness estimation

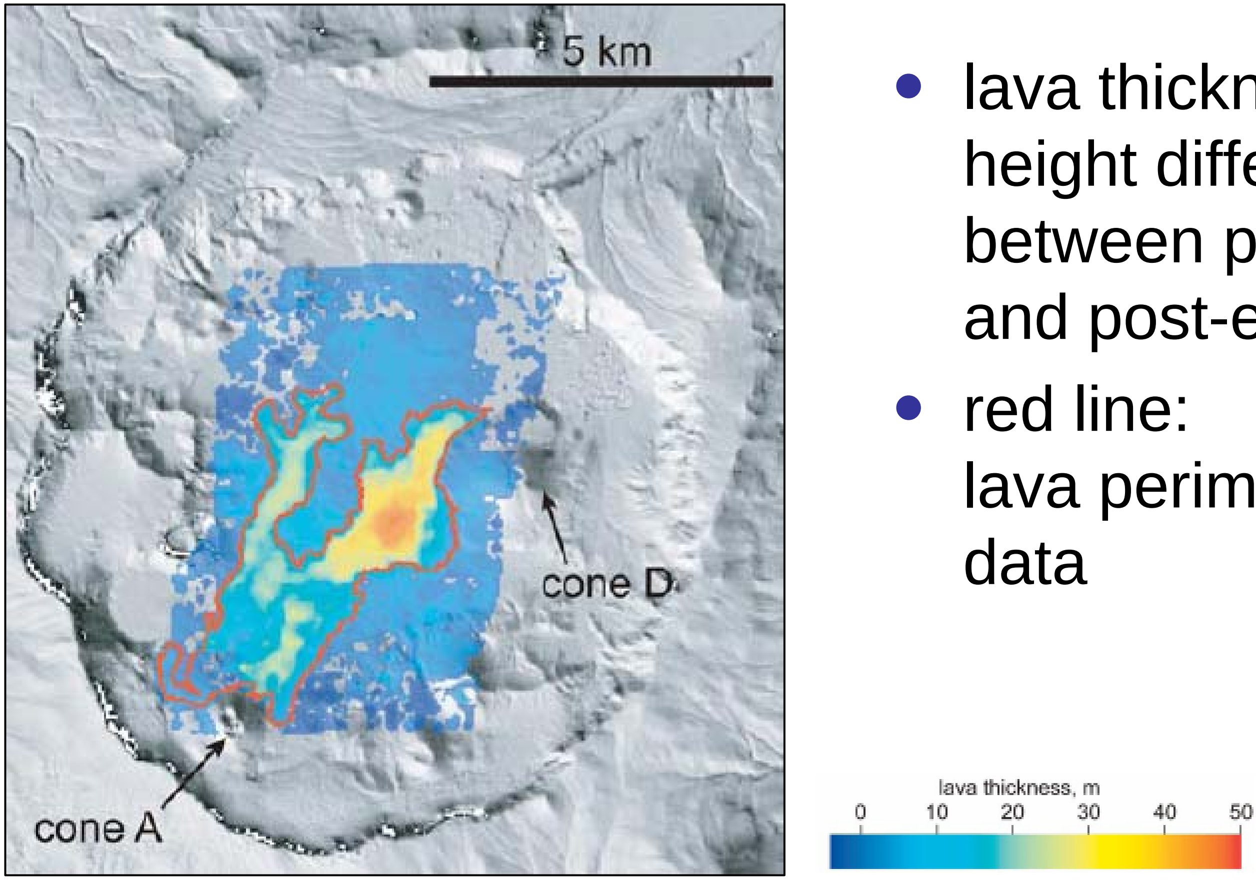

- lava thickness based on height difference between pre-eruption and post-eruption DEMs
- red line: lava perimeter from field data

Lu, Z., Fielding, E., Patrick, M.R. and Trautwein, C.M., 2003. Estimating lava volume by precision combination of multiple baseline spaceborne and airborne interferometric synthetic aperture radar: The 1997 eruption of Okmok Volcano, Alaska. *Ieee Transactions On Geoscience And Remote Sensing*, **41**(6): 1428-1436

Examples: Westdahl and Okmok

Courtesy: Zhong Lu

InSAR images can characterize transient deformation of Westdahl volcano before, during, and after the 1991 eruption

pre-eruption InSAR image

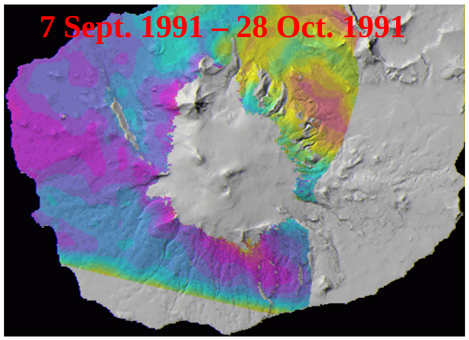

co-eruption InSAR image

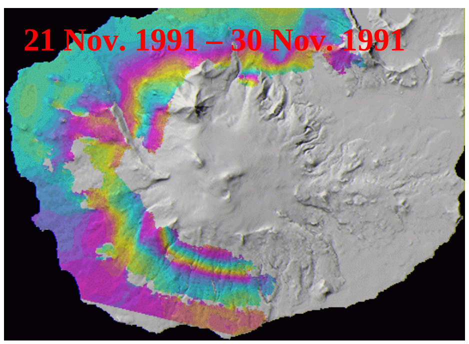

post-eruption InSAR images (several examples)

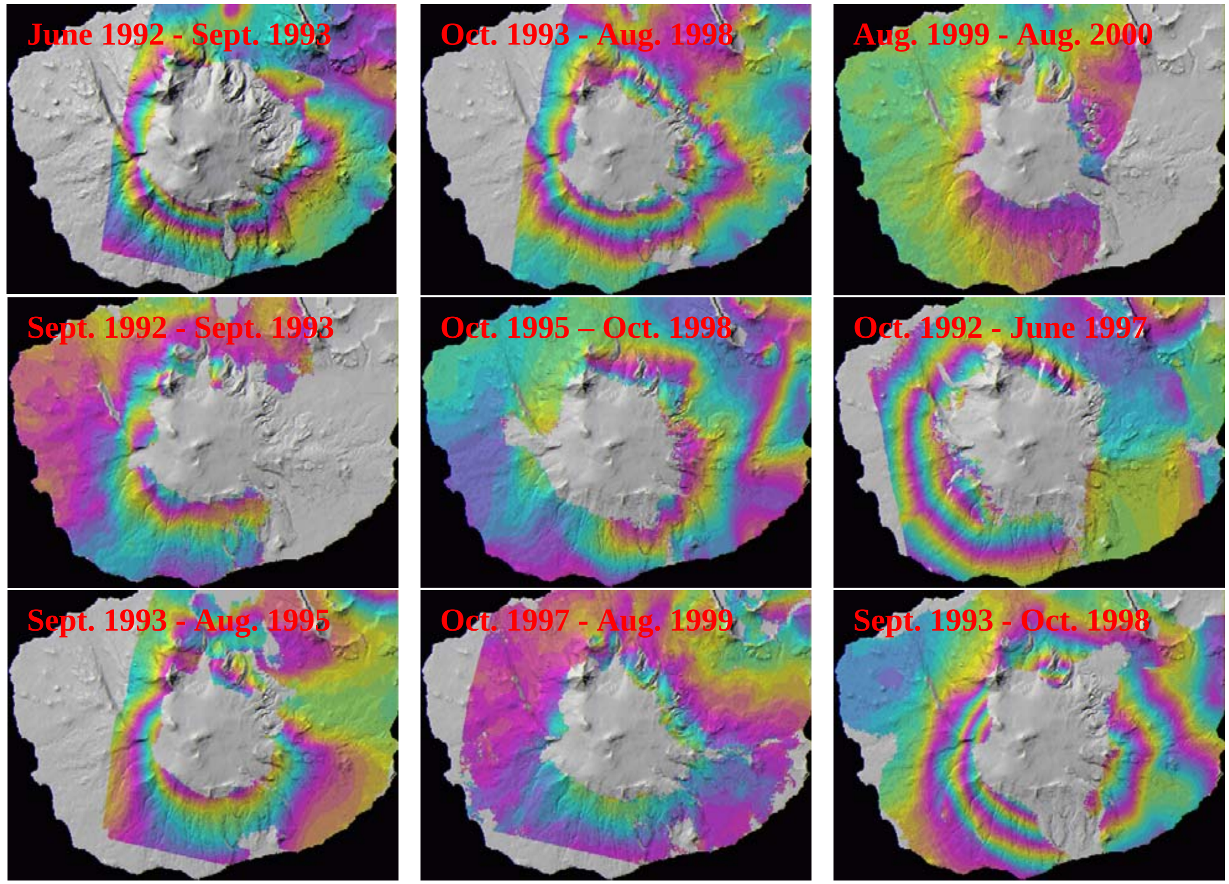

1 color cycle = 2.8 cm deformation

Lu et al., GRL, 2000
Lu et al., JGR, 2003

Deformation history of Westdahl Volcano

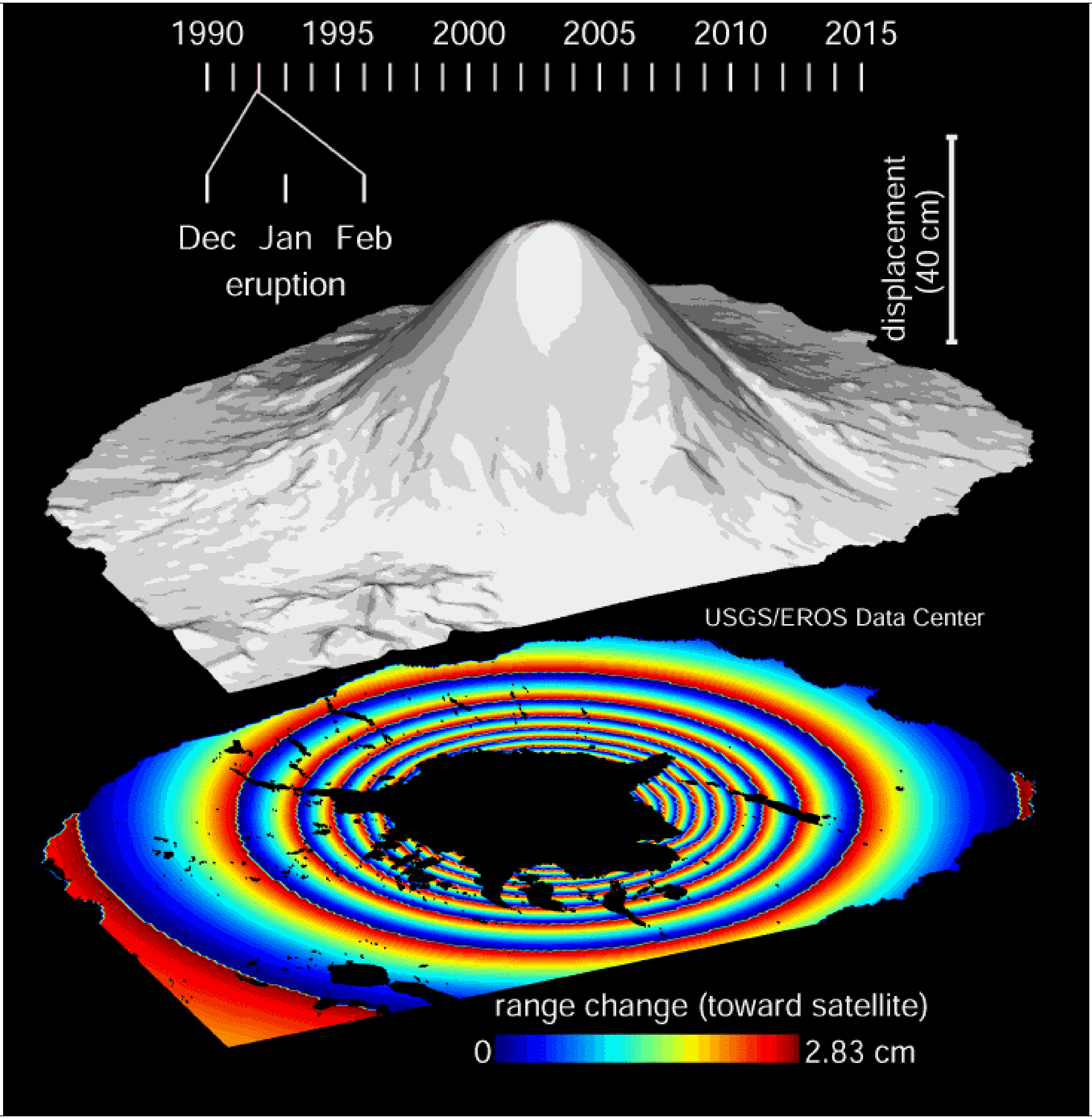

Lu et al., JGR, 2003

InSAR constrains the quantity and timing of magma intrusion

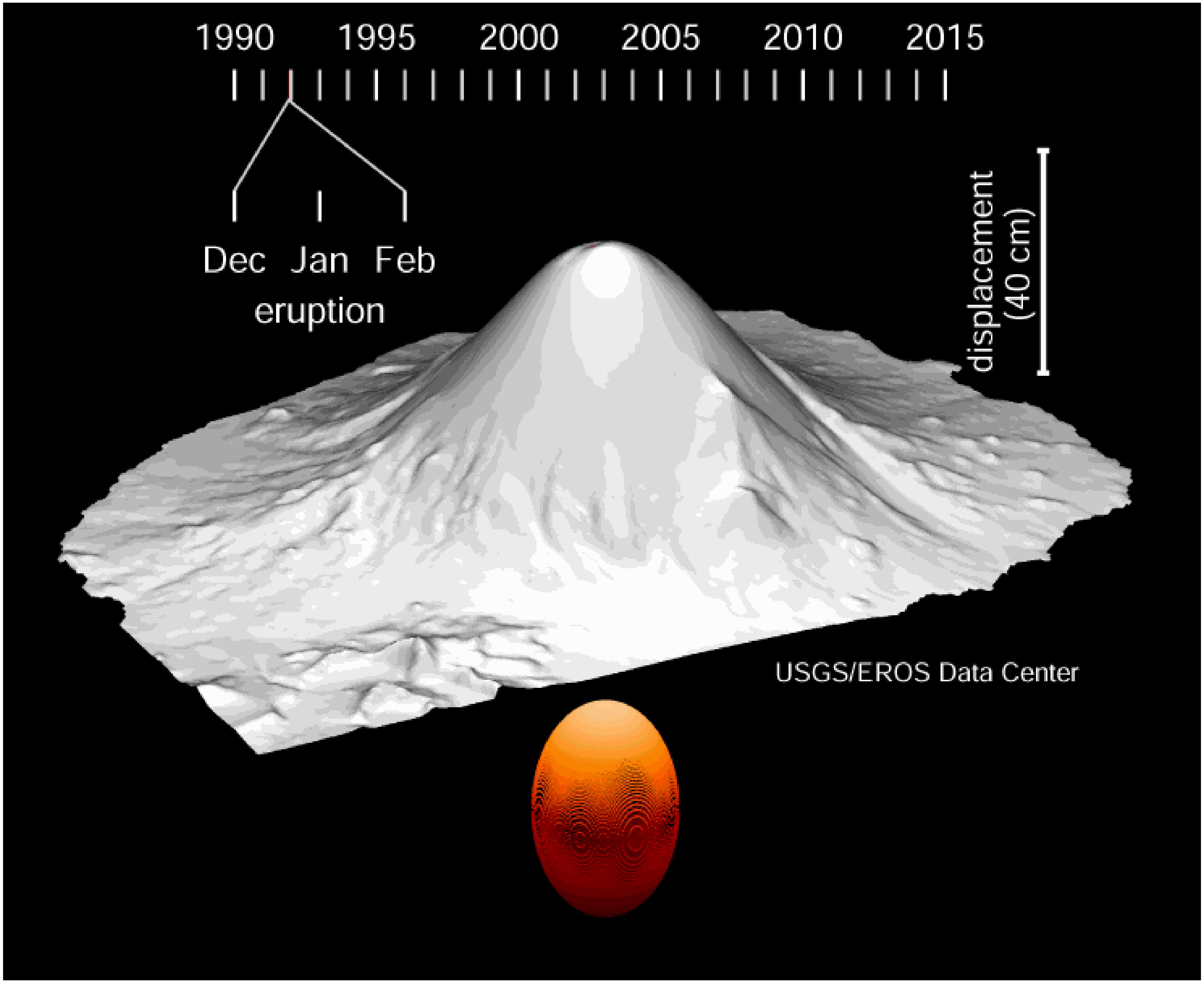

Lu et al., JGR, 2003

Magma plumbing system for Westdahl volcano, inferred from InSAR and modeling

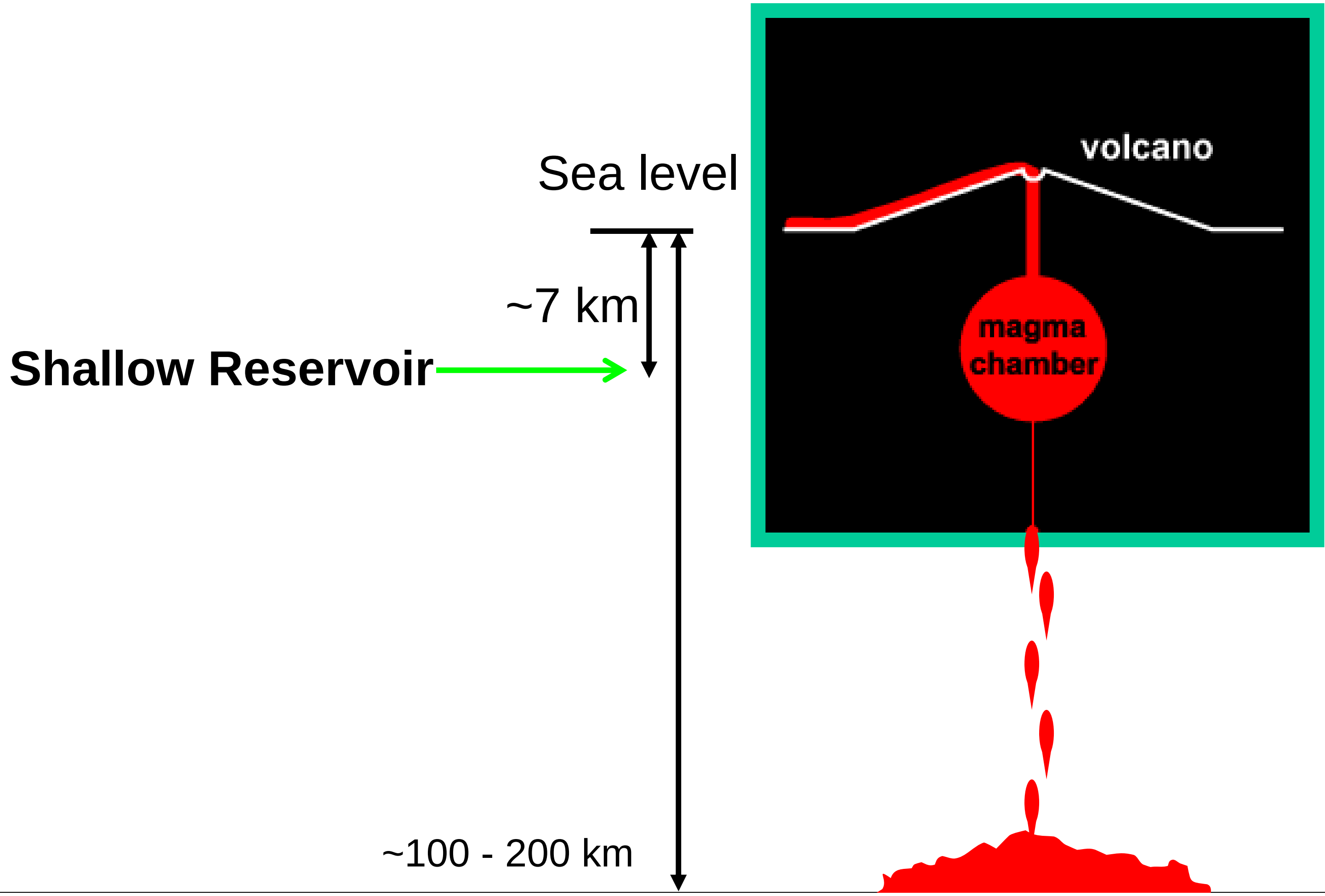

Lu et al., JGR, 2003

Transient deformation of Okmok volcano, Alaska

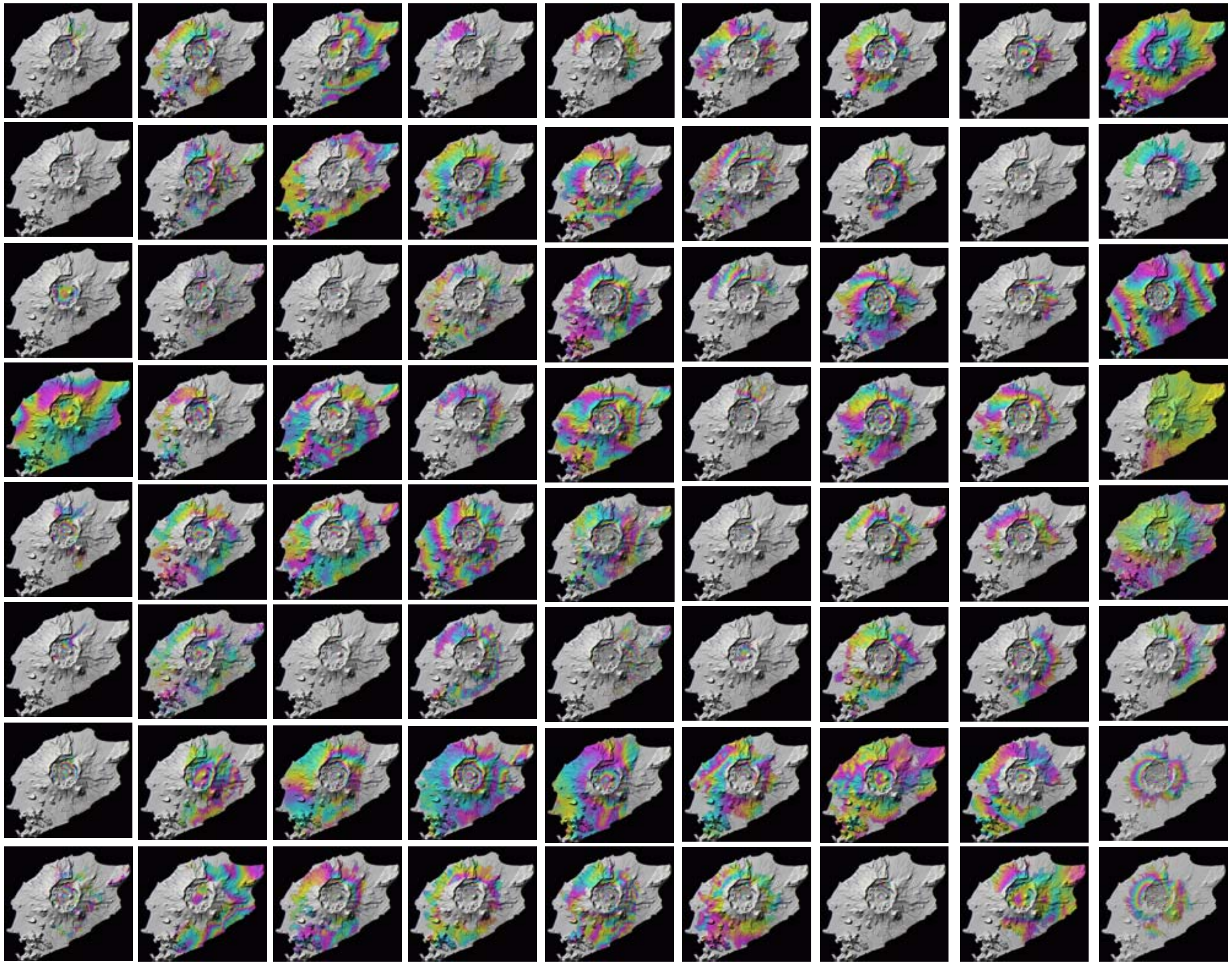

ERS-1:	1992-1996
ERS-2:	1995-2003
Radarsat-1:	2000-2003
JERS-1:	1992-1998

Transient Deformation of Okmok Volcano, Alaska

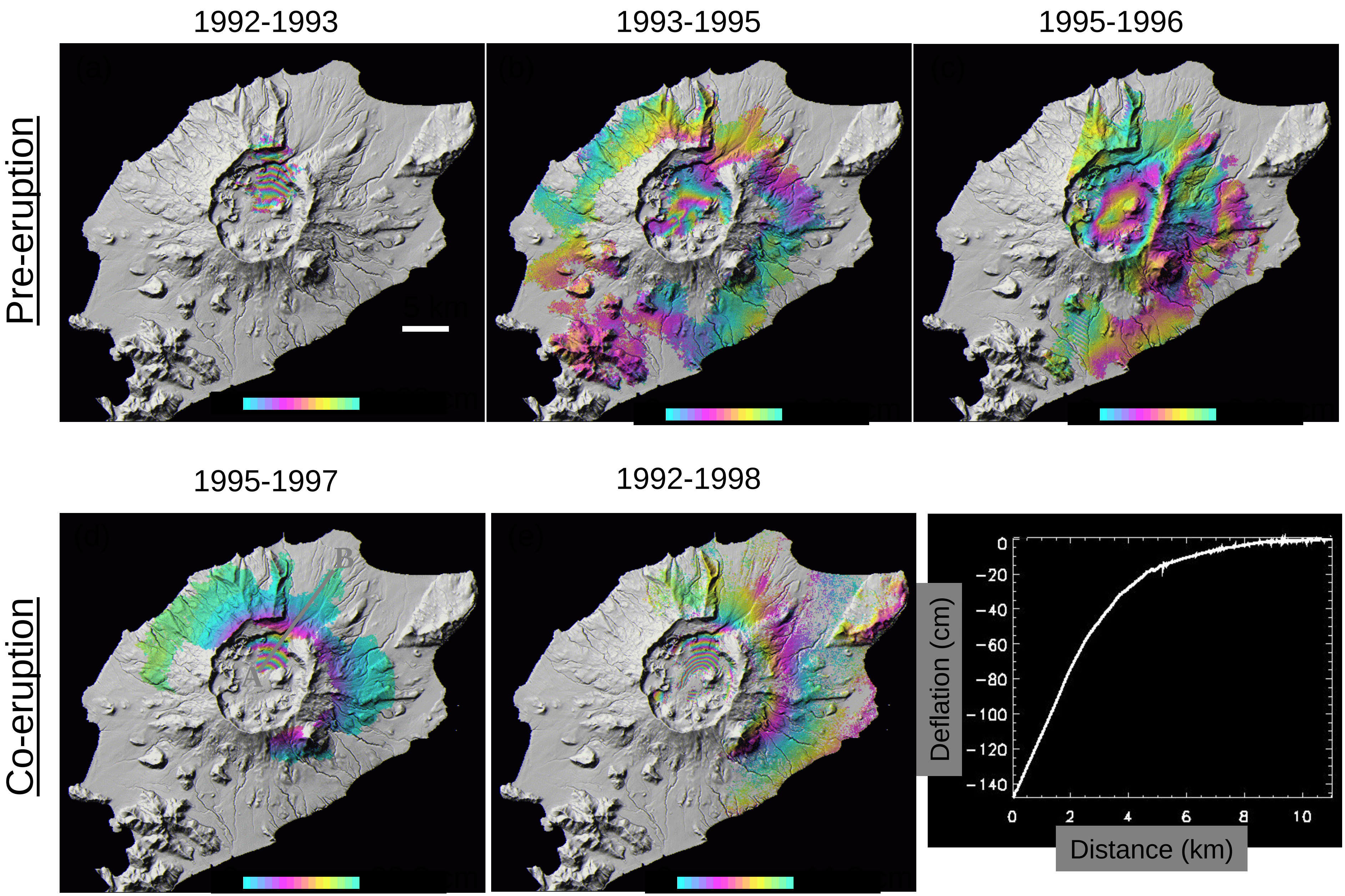

Post-eruptive inflation of Okmok volcano, Alaska

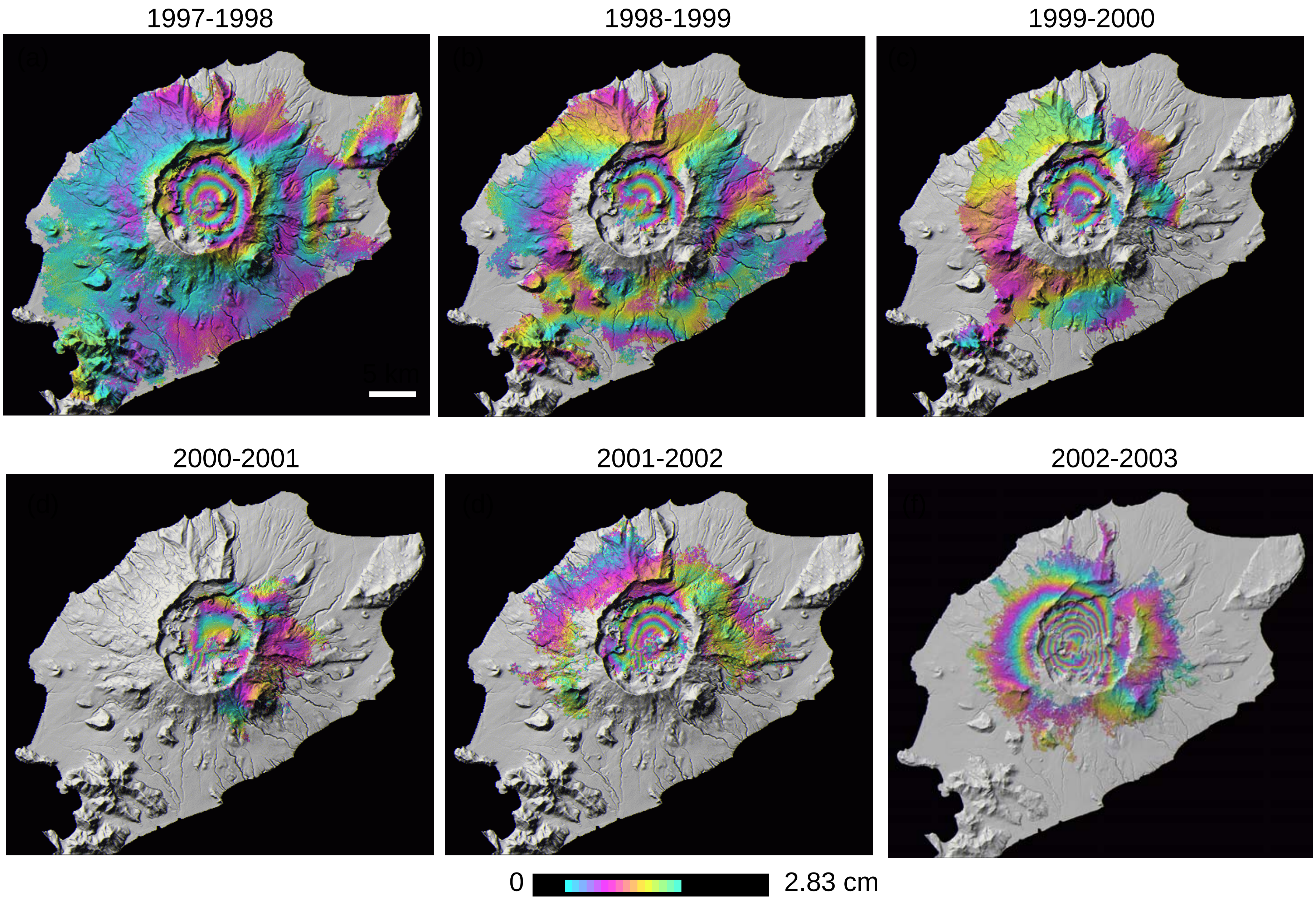

Deformation model → InSAR images:

point expansion source

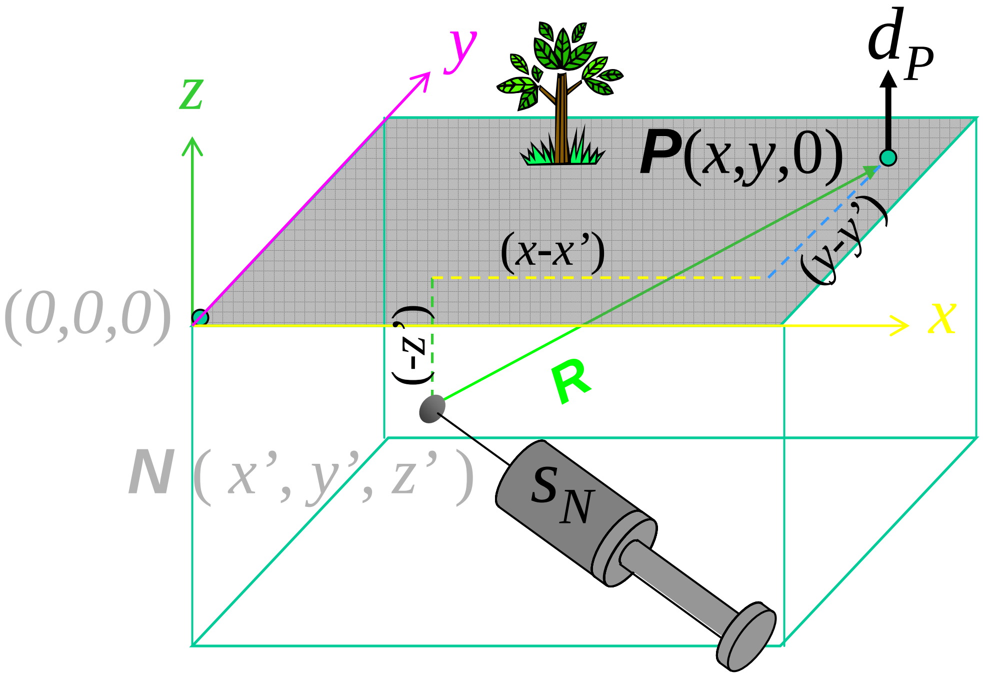

$$\mathbf{R} = \sqrt{[\,(x-x')^2 + (y-y')^2 + (-z')^2\,]}$$

$$d_P = s_N \left(\frac{-z}{R^3} \right)$$

vertical displacement (d_P)

source strength (s_N)

Magma supply rate for the shallow reservoir

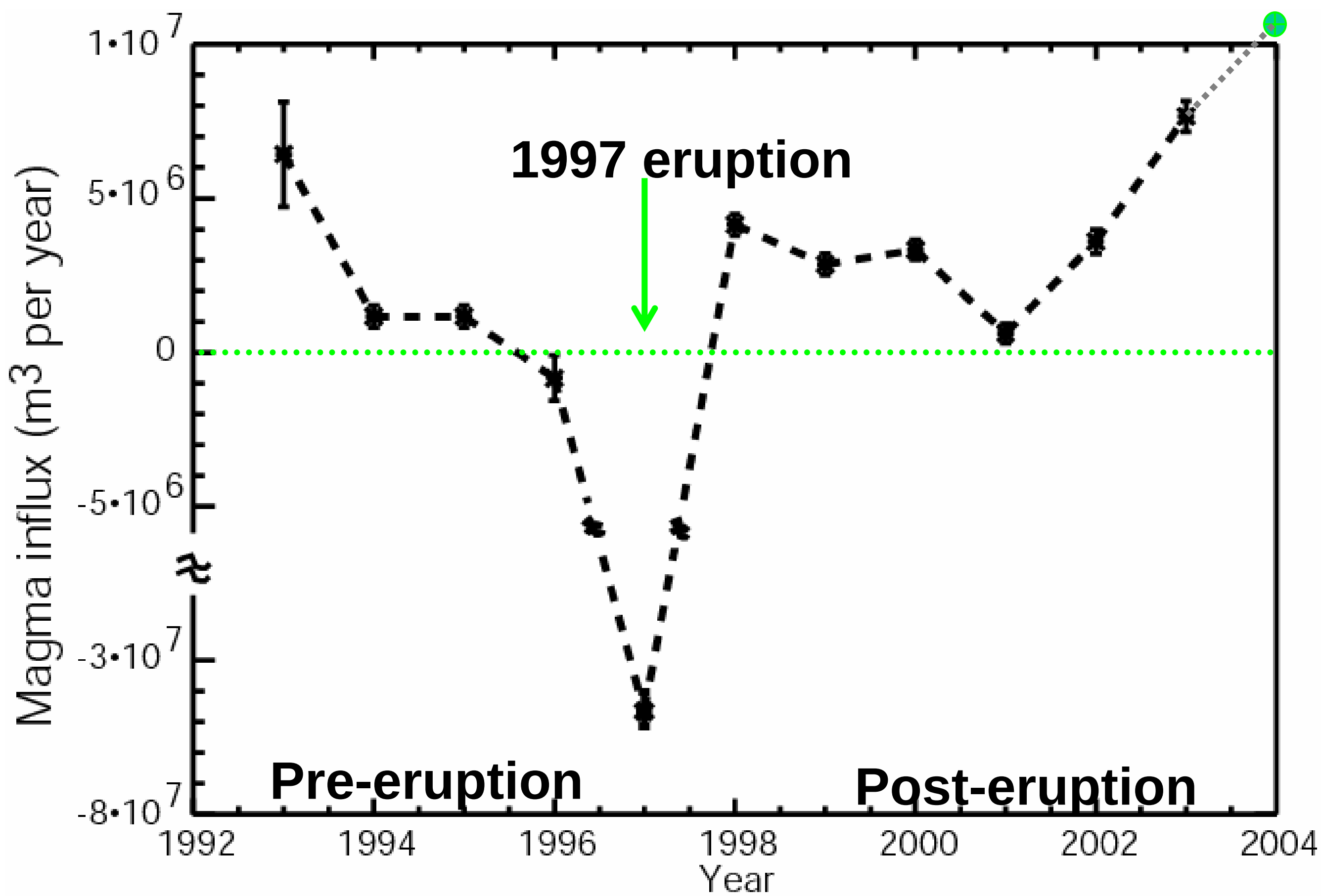

- A magma reservoir residing at 3.2 km beneath the center of the caldera, is responsible for the observed deformation before, during and after the 1997 eruption.

- By the summer of 2004, 45~75% of the magma volume from the 1997 eruption had been replenished.

Deformation of lava flows erupted before 1997

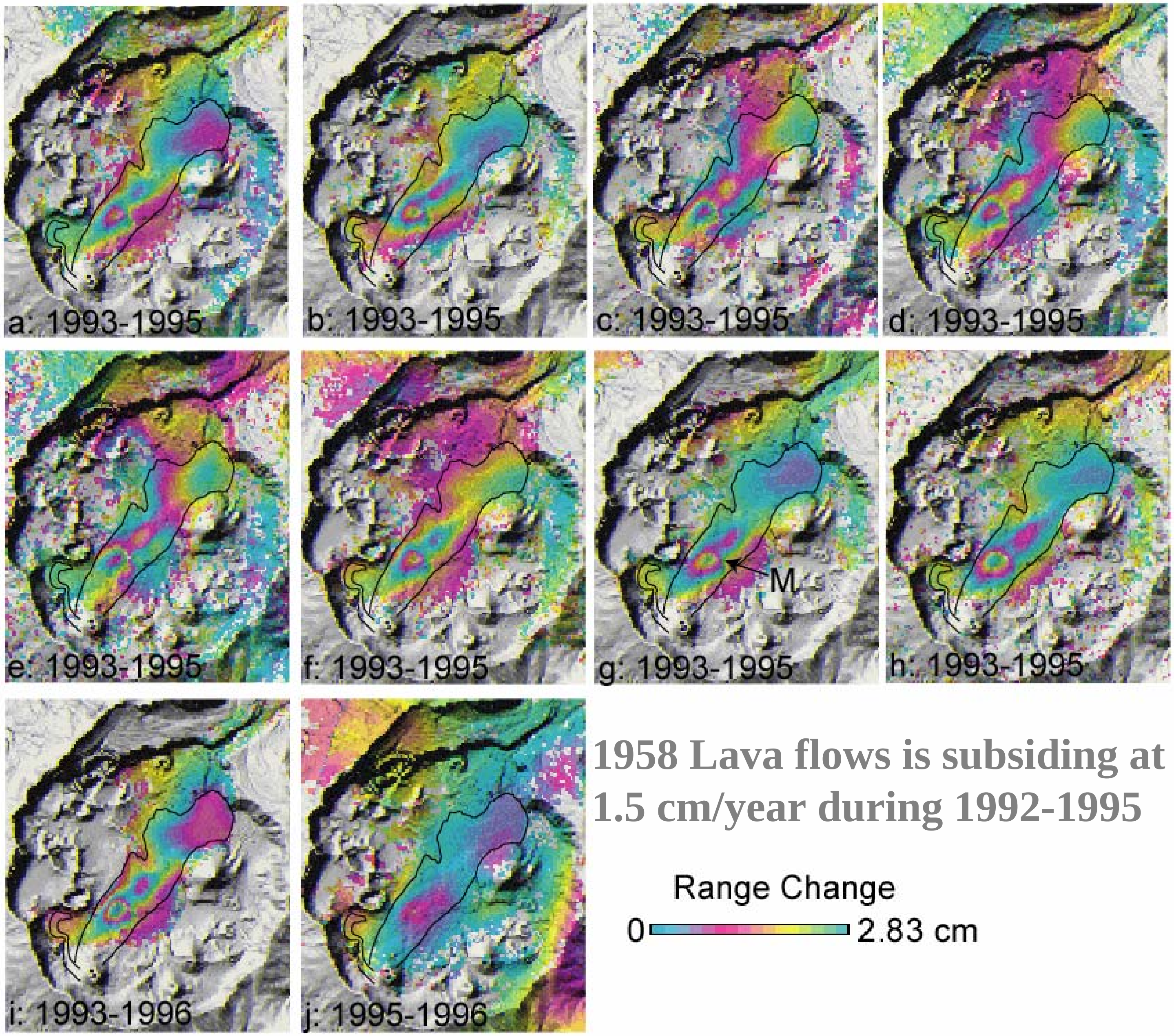

1958 Lava flows is subsiding at 1.5 cm/year during 1992-1995

Deformation of lava flows after 1997 eruption

C-band Images

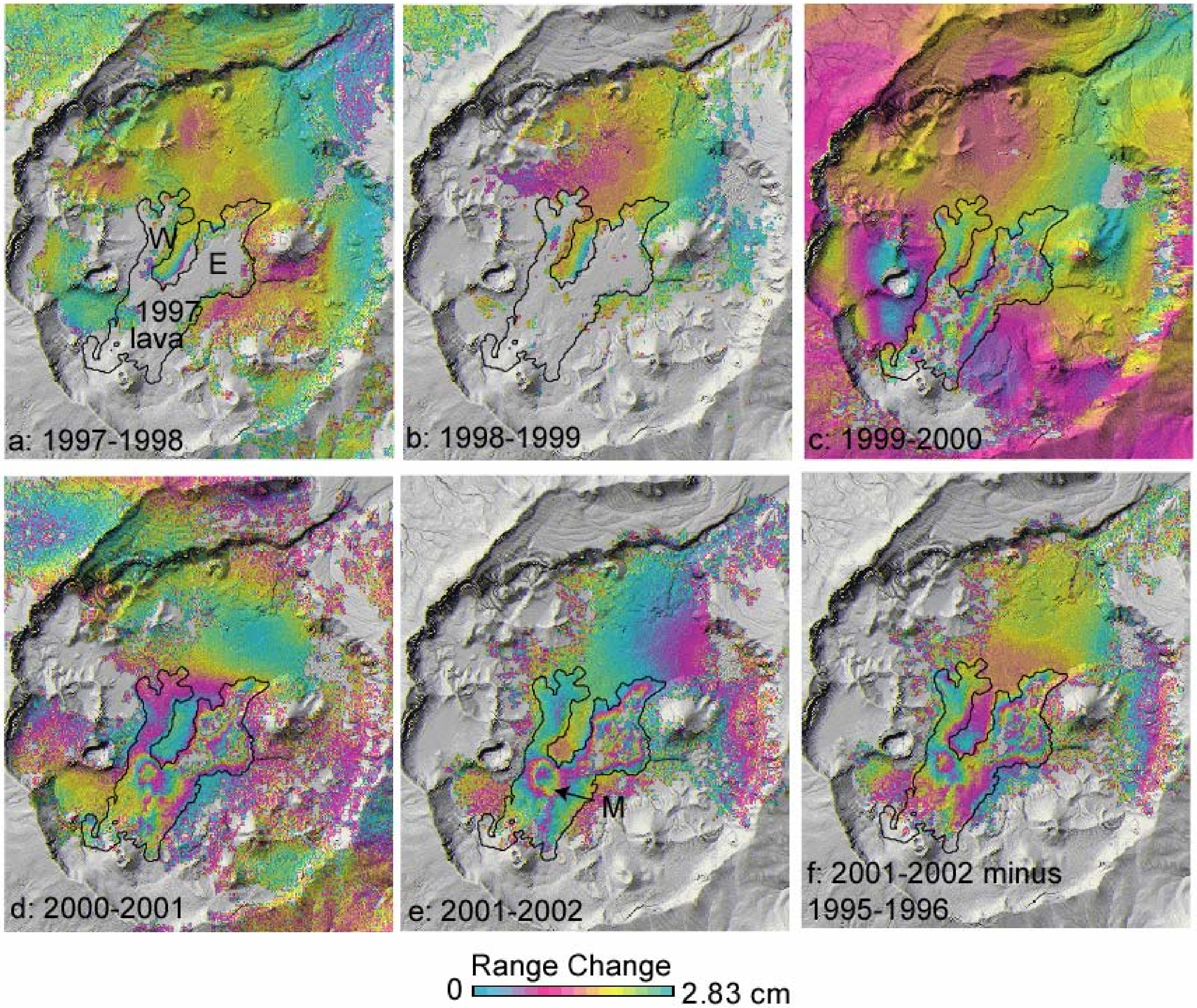

Deformation of 1997 lava flows from JERS-1 Imagery

L-band Images

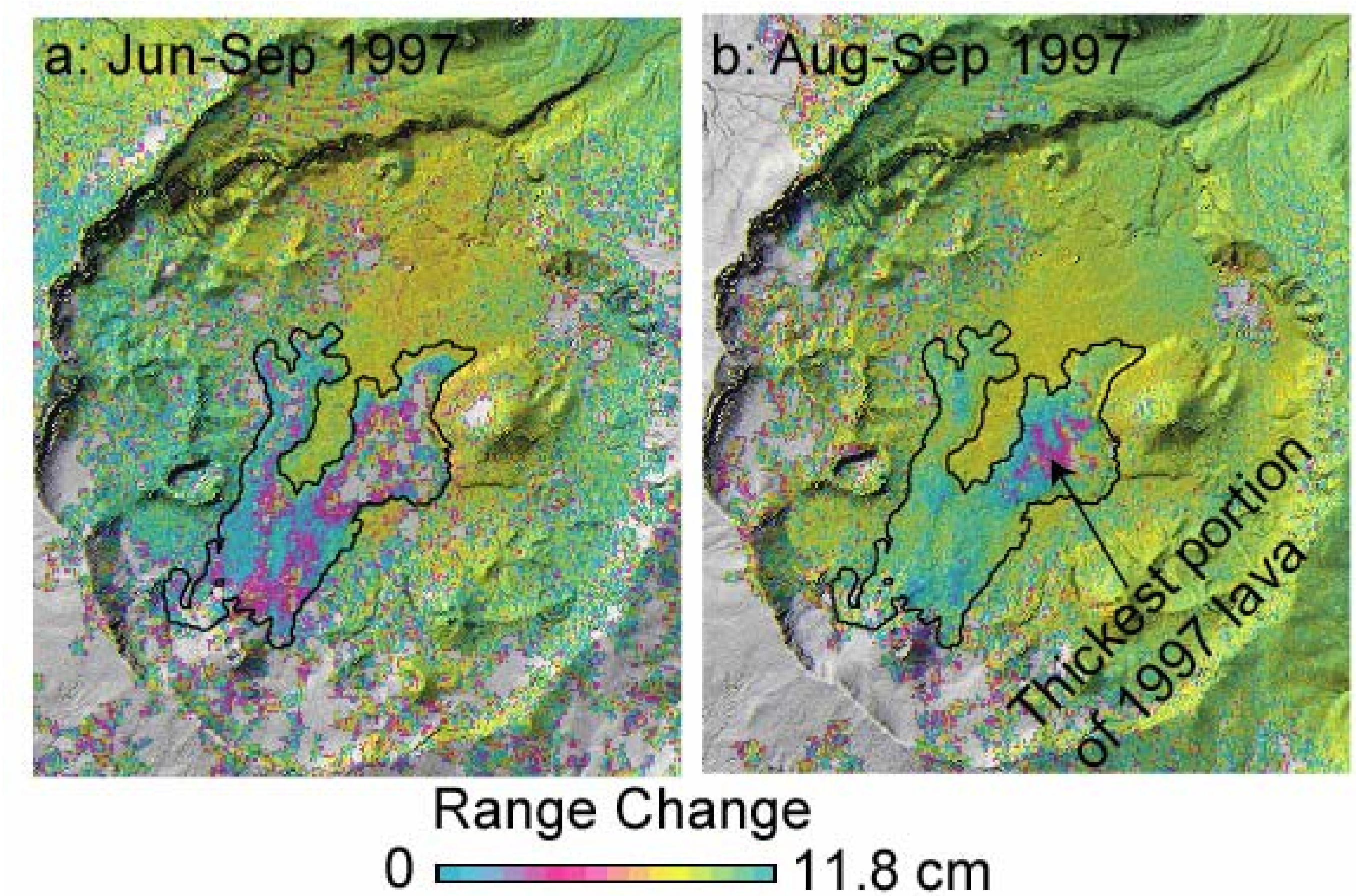

Surface displacement due to lava contraction and consolidation can be 2 mm/day or more four months after the emplacement

Deformation fields of Okmok volcano

Interferograms after the 1997 eruption suggest at least four distinct deformation processes:

1. volcano-wide inflation due to replenishment of the shallow magma reservoir,
2. subsidence of the 1997 lava flows due to thermal contraction,
3. deformation of the 1958 lava flows due to loading by the 1997 flows, and
4. continuing thermal contraction of 1958 lava flows buried beneath 1997 flows.